Mechanics of Advanced Composite Structures 10 (2023) 55 – 68

Semnan University

Mechanics of Advanced Composite Structures

journal homepage: http://MACS.journals.semnan.ac.ir

Buckling Analysis of Functionally Graded Sandwich Beam Based on Third-Order Zigzag Theory

S. Gupta *, **HD. Chalak**

Department of Civil Engineering, National Institute of Technology, Kurukshetra, 136119, India

KEYWORDS

Buckling analysis;
Zigzag theory;
Power law;
Exponential law;
Functionally graded material.

ABSTRACT

In this paper buckling response of a sandwich (SW) beam containing functionally graded skins and metal (Type-S) or ceramic core (Type-H) is investigated using a third-order zigzag theory. The variation of material properties in functionally graded (FG) layers is quantified through exponential and power laws. The displacements are assumed using higher-order terms along with the zigzag factors to evaluate the effect of shear deformation. In-plane loads are considered. The governing equations are derived using the principle of virtual work. The model achieves stress-free boundaries unlike higher-order shear deformation theories and is C0 continuous so, does not require any post-processing method. The present model shows an accurate variation of transverse stresses in thickness direction due to the inclusion zigzag factor in assumed displacements and is independent of the number of layers in computing the results. Numerical solutions are arrived at by using three noded finite elements with 7DOF/node for sandwich beams. The novelty of the paper lies in presenting a zig-zag buckling analysis for the FGSW beam with thickness stretching. This paper presents the effects of the power law factor, end conditions, aspect ratio, and lamination schemes on the buckling response of FGM sandwich beams. The numerical results are found to be in accordance with the existing results. The buckling strength was improved by increasing the power law factor for Type S beams while the opposite behavior was seen in type H beams for all types of end conditions. The end conditions played a major role in deciding the buckling response of FGSW beams. Exponential law governed FGSW beam exhibited a little higher buckling resistance for Type S beams, while a little lower buckling resistance was found for Type S beams for almost all lamination schemes and end conditions. Some new results are also presented which will serve as a benchmark for future research in a parallel direction.

1. Introduction

The Buckling phenomenon is a very different structural response than in-plane compression and can lead to catastrophic failure at critical load. It is also a principal mode of failure for slender components like laminated sandwich beams. Recently sandwich (SW) structures having a three-layered architecture are used in abundance because of their attractive properties of high strength-to-weight ratios, high energy absorption, etc [1, 2]. SW structures use the advantages of two or more distinct materials at a time and in one place. For example, the most common SW structure comprising metal and ceramic exhibits both strength and temperature resistance properties. The main drawback of using SW laminated structures is related to the interface of the layers like de-bonding and stress concentration [3, 4]. A proper solution to these problems is using functionally graded material (FGM) having smoothly varied properties in between two widely varied properties of constituted layers. FGM layer(s) can be used as middle or edge layers of SW beams to produce functionally graded sandwich (FGSW) beams.

FGMs are a new class of composites and have found numerous applications in many engineering and biomedical fields such as nuclear projects, the aviation industry, the aerospace sector, defense, the automobile industry,

* Corresponding author. Tel.: +91-8368556502
E-mail address: simmi.nitk@gmail.com

DOI: 10.22075/macs.2022.27831.1421
Received 2022-07-17; Received in revised form 2022-10-10; Accepted 2022-10-21.

electronics, manufacturing, the energy sector, dentistry, orthopedics [5], etc. As FGM is a combination of distinct materials so, through suitable tailoring, a designer can draw the most complicated requisite properties from them. It provides a better option than conventional composites. There are numerous examples of graded structures present in nature such as bones, teeth, skin, leaves, etc [6]. It is a well-known fact that a structural element built by nature carry out all its functions effectively and is irreplaceable in any manner. So, it can be said that FGM is an ideal material for assigning a structure. Although FGM is ideally suited material for all requirements, can't be used everywhere because of the difficulty and cost of production. Earlier it was impossible to attain the variable microstructure, but now with the advent of high-edge technologies, it is possible to generate an FGM. Mostly volume gradient structure is made for an FGM.

The highly heterogeneous structure of FGM causes inflation of shear deformation effects in the thickness direction of SW beams. So its behaviour becomes complex which creates reliability issues in practical applications. So, response data of FGSW structures should be generated and compiled to help in increasing the practical application in various fields.

Many theories are developed for getting the true behaviour of SW beams. An elaborate review of different theories used for analyzing FGSW structures is given by [7]. Elasticity theories [8-12] provide benchmark data by achieving the highest degree of accuracy but they are cumbersome, so many simplified theories based on some assumptions are developed by researchers. When going through the literature two broad categories can be identified for the theories developed. They are equivalent single layer (ESL) and layer-wise theories (LWT). ESL theory assumes the primary variable with reference to the central/neutral layer while LWT assumes the same layer-wise. The order of displacement in independent variable assumption creates different theories like classical plate theories CPT [13-16], First order shear deformation theory FSDT [17-19], third-order shear deformation theory TOT [20], higher-order shear deformation theory HOT [21-23], refined HOT [24-30] and quasi-3D theory [31]. CPT ignores shear deformation effects and overestimates the buckling loads. FSDT requires a correction factor for satisfying parabolic variation of shear deformation. TOT and HOT do not give traction-free shear stresses. These displacement-based theories are applied using ESL or LWT approach. The ESL approach is simple so, is mostly used by researchers.

LWT is more accurate than ESL theory because it has a more realistic approach for multilayered beams having an uneven distribution of dependent variables resulting from a layer-wise construction. LWT is further classified as discrete LWT and zigzag LWT. Discrete LWT [32] assumes the variables with the individual layers, so the solution becomes difficult to achieve for a larger number of layers. Also, most of the discrete LWT does not satisfy the interlaminar stress continuity, since two different values of stresses are built at the interface of these layers from the different elastic modulus of two layers. Zigzag LWT [33-43] describes the nonuniform variation in the dependent variable by including an additional term in the displacement field while adopting the ESL assumption. The superiority of zigzag LWT in getting static and dynamic results over FSDT and TOT is listed by Kapuria et al. [37]. By comparing zigzag LWT with benchmark elasticity results for SW beams, he found it gives the least percentage of errors. The manner by which the zig-zag LWT is able to satisfy the interlaminar displacement continuity of laminated structures is well cited by [41].

Pandey and Pradyumna [32] analyzed the FGSW plate by employing eight noded C^0 isoparametric finite elements having 13DOF using a layer-wise expansion for displacement fields. Chakrabarty et al [38] defined the issue of C1 continuity associated with implementing the finite element method using the zig-zag theory and solved the buckling problem of the SW beam. Averil [33] developed first-order zig-zag formulations for laminated beams and employed a penalty function to alleviate the C1 requirement for two noded finite elements. Later Cho and Averill [34] used sublaminate approximation to avoid the C1 requirement for four noded elements. Vo et al [24] used a linear interpolation function in generalized displacements to solve the C1 continuity issue. Neves [36] used the meshless method in place of FEM to solve the buckling problem of FGM sandwich beams. Kapuria and Ahmed [42] used interdependent interpolation. In the present work problem of C0 continuity arising from the use of zigzag theory in combination with FEM for getting solutions is avoided by expressing the derivation terms of shear stress in terms of other variables and solving the equations. It does not require any post-processing method.

Solving a problem involves two main steps: consideration of a theory and the type of solution method. Until now most researchers have used ESL theories for simplicity. This paper uses an advanced theory that overcomes all the deficiencies of earlier proposed theories as overestimating the buckling loads (CPT); requiring a shear correction factor for correctly assessing the variation of shear stresses (FSDT); providing the actual parabolic variation of transverse shear stresses, but not fulfilling stress-free boundary conditions (HOT); providing a solution which is dependent on the number of layers and giving two values of shear stress at the interface because of the two different displacement equations in adjacent layers (LWT). The zigzag theory used in this work is supreme to all the above-stated theories as it does not need any shear correction factors, provides the actual parabolic variation of transverse shear stresses, fulfills stress-free boundary conditions, and is not dependent on the number of layers for the solution. The only issue in using Zigzag theory is the problem of C0 continuity due to the inclusion of additional terms in displacement approximation, which is avoided here as discussed earlier.

Based on the literature review, authors found that plenty of study is available for the structural response of FG sandwich beams based on analytical approach such as Navier's solution, because of its accuracy and ease in finding solutions, but has restraint in terms of boundary conditions, material law, loading conditions, etc. These restraints are overcome by using numerical methods like FEM, meshfree method, etc. In this study a numerical method: FEM is employed to study the response of symmetric and asymmetric FGSW beams subjected to various end conditions and material laws. Sayyad and Ghugal [43] reported that an ample amount of research is available for the analysis of plates and bending and vibration response SW structures while buckling analysis of FGSW beams is very less studied. Although a sufficient amount of literature is present on the zig-zag analysis of SW structures; but till now very less authors have taken up the zig-zag method for analyzing FGSW beams because of the complexity in arriving at the solutions due to the inclusion of the zig-zag factor along with FGM layer(s). Among the zig-zag analysis-based studies, to the author's best knowledge, buckling analysis is not available and the bending and vibration studies do not adopt the numerical solution method, nor take into account the thickness stretching effects. The novelty of the present paper is presenting the buckling analysis results for the FGSW beam using a zig-zag theory with thickness stretching through a numerical method (FEM). Present paper deals with finding buckling responses of FGSW beams for various end conditions, aspect ratios, and homogenization laws based on the recently proposed zig-zag theory [38]. The present theory satisfies interlaminar stress continuity. A C0 continuous FEM formulation of 3 noded elements with 7DOF/node is used. The present paper also gives new results which will serve as a benchmark for future works with a similar vision.

2. Modeling of Material Properties

A three-layered SW beams (Fig 1) of two types: Type P and Type E are synthesized. These are further classified according to the core material: Type P-H, E-H (hardcore) (Fig 2a), and Type P-S, E-S (softcore) (Fig 2b) for analysis. These beams have FGM as face sheets and cores built as ceramic (Type H) and metallic (Type S). As it is established that the material property consideration has a great effect on the analysis results, so this study uses two types of material modeling (power law and exponential law) and the results were compared. Material property variation is modeled in two ways:

2.1. Power law:

Garg et al. [44] presented a review of the analysis of FGM sandwich structures and prepared a list of literature based on the type of material law used. They found that more than 90% of the FGM-related literature used power law for estimating the material properties as it is simplest as per the ease of use. A similar observation was made by Swaminathan et al. [45]. In this paper, material properties are graded in the thickness direction according to the power-law distribution in terms of the volume fractions of the constituents of the material, and the effective material properties are estimated on the basis of the Voigt model as the homogenization method. Although the Voigt rule does not consider the interaction among adjacent inclusions, Mori–Tanaka method considered these interactions of neighboring phases at the microscopic level as done in [46,47]. Using Voigt model material property in FGM, P(z) is expressed as:

$$P(z) = P_m + (P_c - P_m)V_c \qquad (1)$$

where P_m and P_c are material properties of metal and ceramic and their variation is shown in Fig. 3 for a lamination scheme of 2-2-1. V_c is the volume fraction of the ceramic part which is written as: (For Type P beams)

$$V_c = \left(\frac{z-h_0}{h_1-h_0}\right)^n \qquad \text{for } z\epsilon[h_0, h_1]$$

$$V_c = 1 \qquad \text{for } z\epsilon[h_1, h_2]$$

$$V_c = \left(\frac{z-h_3}{h_2-h_3}\right)^n \qquad \text{for } z\epsilon[h_2, h_3]$$

2.2. Exponential law:

The FGM part is made to obey exponential law and the variation of material property by this law is shown in Fig. 4 for a lamination scheme 2-2-1and is written as:

$$P(z) = P_m \mathrm{e}^{\left(\ln\left(\frac{P_c}{P_m}\right)V_c\right)} \qquad (2)$$

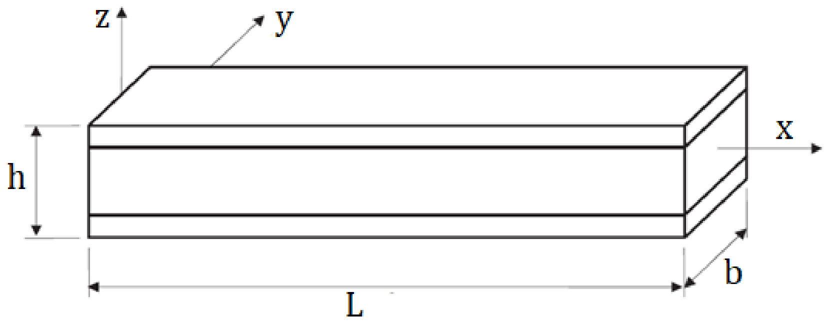

Fig. 1. Geometry of sandwich plate in the Cartesian coordinate system

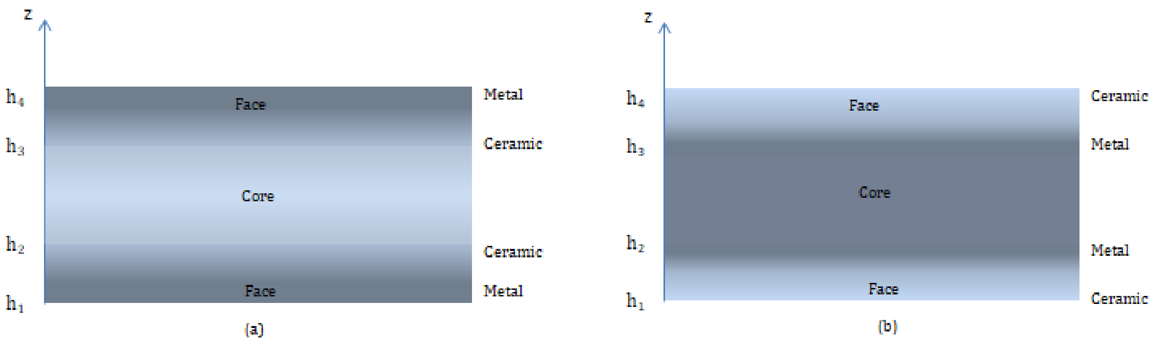

Fig. 2. Layer configurations of FGSW beam of various types (a) Type P-H and Type E-H (b) Type P-S and Type E-S

where V_c is given as: (For Type E beams)

$$V_c = \left(\frac{2z+1}{2h_1+1}\right)^n \qquad \text{for } z\epsilon[h_0, h_1]$$

$$V_c = 1 \qquad \text{for } z\epsilon[h_1, h_2]$$

$$V_c = \left(\frac{2z-1}{2h_2-1}\right)^n \qquad \text{for } z\epsilon[h_2, h_3]$$

3. Theoretical Formulations

Consider a beam in the assumed coordinate system shown in Fig 1. The displacement in x (u_x) direction is assumed as:

$$u_x = u_0 + z\varphi^x + z^2\zeta^x + z^3\chi^x + \sum_{i=1}^{n_u-1}(z - z_i^u)\, H(z - z_i^u)\psi_i^{xu} + \sum_{i=1}^{n_l-1}(z - z_i^l)\, H(z - z_i^l)\psi_i^{xl} \tag{3}$$

where u_0 is mid-plane displacement along the x-axis for any point in the SW beam, φ^x is the rotation of normal to mid-plane and n_u, n_l depict the number of upper and lower layers, respectively. ζ^x, χ^x are higher-order unknowns, and ψ_a^{xu}, ψ_b^{xl} are the slope of a-th and b-th layers corresponding to the upper and lower layers respectively. $H(z - z_a^u)$ denotes unit step function. The displacement in z-direction (u_z) is assumed as taken in [38] as:

$$u_z = l_1 w_u + l_2 w_0 + l_3 w_l \text{ for core}$$
$$= w_u \quad \text{for upper face layer} \tag{4}$$
$$= w_l \quad \text{for lower face layer}$$

where w_u, w_0 and w_l are the values of the transverse displacement at the top, middle and bottom lamina of the core, respectively, and l_1, l_2 and l_3 are Lagrangian interpolation functions in the z-direction. By taking the reference of [38], the constitutive relation for stress in local coordinates (σ_l) of k-th lamina is given as:

$$\sigma_l = [C_k]\epsilon_l \tag{5}$$

where $[C_k]$ is transformed rigidity matrix of k-th lamina and σ_l appeared in the above equation can be converted into a global coordinate system by using the transformed compliance matrix$[\hat{C}]$ as:

$$\{\bar{\sigma}\} = [\hat{C}_k]\{\bar{\epsilon}\} \tag{6}$$

Now using the conditions of zero transverse shear stress at z=h/2 and z=-h/2 and transverse shear stress continuity at interfaces of layers with at z=h/2, $u = u_l$ at z=-h/2, $u = u_u$.

The terms $\zeta^x, \chi^x, \psi_i^{xu}, \psi_i^{xl}$, $(\partial w_u/\partial x)$ and $(\partial w_l/\partial x)$ are expressed in terms of displacement u_0, u_u, u_l and φ^x as:

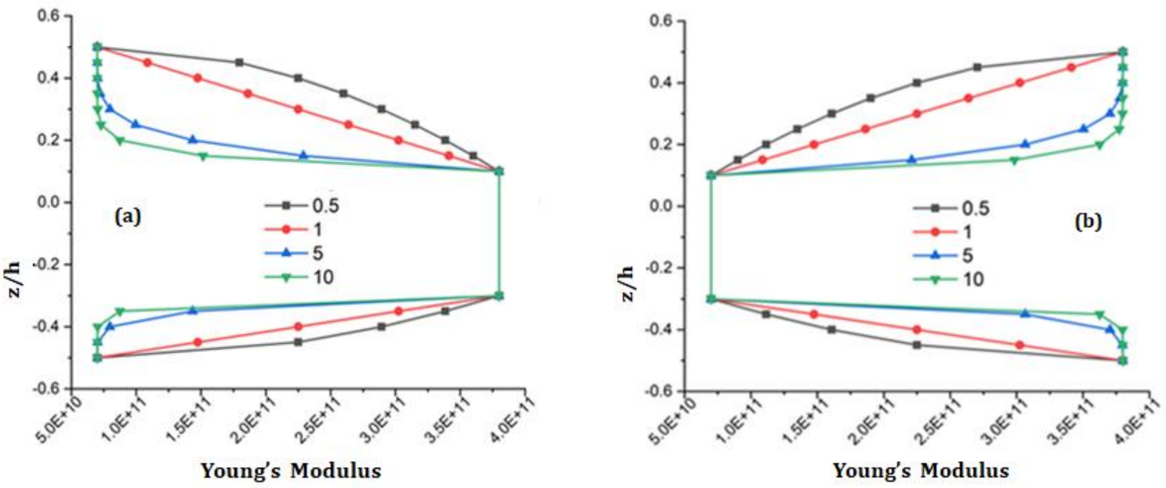

Fig. 3. Variation of material property across the thickness of 2-2-1 FGSW beam (a) Type-P-H (b) Type P-S

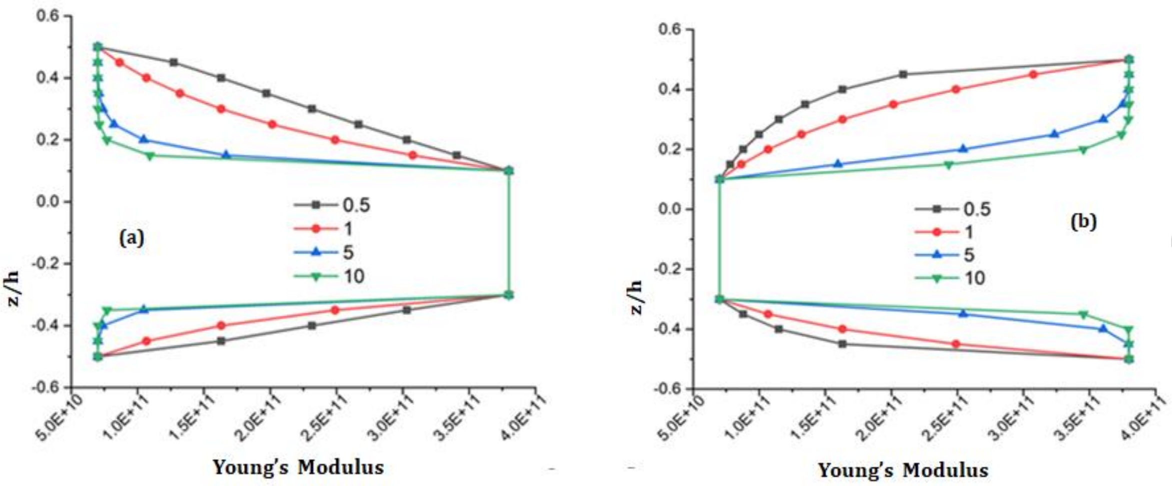

Fig. 4. Variation of material property across the thickness of 2-2-1 FGSW beam (a) Type E-H (b) Type E-S

$$M = [N]\{\eta\} \tag{7}$$

where $\{M\} = \{\zeta^x, \chi^x, \psi_i^{xu}, \psi_i^{xl}, (\partial w_u/\partial x), (\partial w_u/\partial x)\}^T$, $\{\eta\} = \{u_0, u_u, u_l, \varphi^x\}^T$ and material properties determine elements of $[N]$. Through Equation (7) we are able to write the differentiation of transverse displacements in terms of other unknowns, thus avoiding the C1 continuity issue. Now Equation (3) is rewritten as:

$$u_x = f_1 u_0 + f_2 \varphi^x + f_3 u_u + f_4 u_l \tag{8}$$

where the coefficients of $f_i's$ are determined by values of z, H, and material properties. Now, when all the coefficients of higher order terms of Equation (3) are eliminated so, we can write the generalized displacement with the help of Equations (4) and (8) as:

$$\{\delta\} = \{u_0 w_0 \varphi^x \; u_u w_u u_l w_l\}^T \tag{9}$$

Writing strain field in terms of unknowns as a combination of linear and nonlinear parts by using strain-displacement connection and Equations (3-6) as:

$$\{\bar{\varepsilon}\} = \{\bar{\varepsilon}\}_L + \{\bar{\varepsilon}\}_{NL} \tag{10}$$

where the linear part of the strain is

$$\{\bar{\varepsilon}\}_L = \left[\frac{\partial u_x}{\partial x} \frac{\partial u_z}{\partial z} \frac{\partial u_x}{\partial z} + \frac{\partial u_z}{\partial x}\right] \quad \text{or} \quad \{\bar{\varepsilon}\}_L = [H]\{\varepsilon\} \tag{11}$$

and nonlinear part of strain is:

$$\{\bar{\varepsilon}\}_{NL} = \{1/2(\partial \bar{u}_z/\partial x)^2 + 1/2(\partial \bar{u}_x/\partial x)^2\} \qquad \{\bar{\varepsilon}\}_{NL} = 1/2\,[A_G]\{\theta\} \tag{12}$$

where, $\{\theta\} = [\partial \bar{u}_z/\partial x \;\; \partial u_x/\partial x]$ or $\{\theta\} = [H_G]\{\varepsilon\} = [H_G][B]\{\delta\}$ and

$$\{\varepsilon\} = \begin{bmatrix} u_0 \varphi^x u_u u_l w_u w_0 w_l (\partial w_u/\partial x)(\partial w_0/\partial x)(\partial w_l/\partial x) \\ (\partial u_0/\partial x)(\partial \varphi^x/\partial x)(\partial u_u/\partial x)(\partial u_l/\partial x) \end{bmatrix}$$

And the elements of matrices $[H]$, $[A_G]$, and $[H_G]$ are dependent on z and unit step functions. The data $l_1, l_2, l_3, f_i's$ and the elements of $[H]$ can be accessed by the corresponding author through the mail.

Now applying the virtual work principle on the same lines as done in [35], the total potential energy of the system is given as :

$$\Pi_e = E_S - E_{ext} \tag{13}$$

where E_S is the strain energy and $E_{ext}$is the energy due to externally applied load. Utilizing equations (5) and (9), the strain energy is

$$E_S = \frac{1}{2}\sum_{k=1}^{n} \iint \bar{\varepsilon}^T\, [\bar{Q}_K]\, \{\bar{\varepsilon}\} dxdz = \frac{1}{2}\int \{\bar{\varepsilon}\}^T\, [D]\{\varepsilon\} dx \tag{14}$$

where

$$D = \frac{1}{2}\sum_{k=1}^{n} \int [H]^T\, [\bar{Q}_k]\, \{H\} dz \tag{15}$$

E_{ext} is computed as:

$$E_{est} = \frac{1}{2}\sum_{k=1}^{n} \iint \{\bar{\varepsilon}\}_{NL}^T\, [S^i]\, \{\bar{\varepsilon}\}_{NL} dxdz = \frac{1}{2}\int \{\bar{\varepsilon}\}_{NL}^T\, [G]\{\bar{\varepsilon}\}_{NL} dx \tag{16}$$

where $= \sum_{k=1}^{n} \int \{H_G\}^T [S^i] \{H_G\} dz$ and $[S^i]$ is the stress matrix of the i-th layer generated from the external in-plane loads which is given as $[S^i] = \begin{bmatrix} 6_x & 0 \\ 0 & 0 \end{bmatrix}$

4. Finite element Formulations

A numerical method i.e., FEM is used for the solution of buckling problems. A quadratic element with three nodes and seven degrees of freedom is considered.

The generalized displacement vector δ at any point can be expressed in terms of displacement δ_i and shape functions N_i related to i-th node.

$$\{\delta\} = \sum_{i=1}^{n} N_i \{\delta\}_i \tag{17}$$

Here, n is no. of nodes in one element. From Equation (17), the strain vector $\{\varepsilon\}$ used in Equation(11) is given as:

$$\{\varepsilon\} = [B]\{\delta\} \tag{18}$$

where [B] is the strain displacement matrix.

The potential energy given in Equation (13) can be rewritten by using Equations (14-16) as:

$$\Pi_e = 1/2 \int \{\delta\}^T\, [B]^T [D][B]\{\delta\} dx - 1/2 \int \{\delta\}^T [B]^T [G][B]\{\delta\}\, dx = 1/2\{\delta\}^T [K_e]\{\delta\} - 1/2\lambda\{\delta\}^T [K_G]\{\delta\} \tag{19}$$

where,

$$[K_e] = \int [B]^T\, [D][B] dx \tag{20}$$

$$[K_G] = \int [B]^T\, [G][B] dx \tag{21}$$

Finally minimizing $\Pi_e$with respect to {δ}

$$[K_e]\{\delta\} = \lambda[K_G]\{\delta\} \tag{22}$$

where $[K_e]$and $[K_G]$ are stiffness matrix and geometrical stiffness matrix and λ is the buckling load factor. A flow chart is made by incorporating all the steps needed to be followed for determining λ, which is given in the appendix. A code is written in FORTRAN for calculating the λ. A simultaneous iteration method is utilized for solving the buckling Equation (22).

5. Results and discussions

Buckling analysis for four types of FGSW beams is presented here for the materials having properties: Ceramic (Al2O3) Ec=380GPA, μ=0.3 and Metal (Al) Ec=70 GPA, μ=0.3. The Non-dimensional factor used in this study is given as:

$Non\ dimensional\ Buckling\ load, \bar{\lambda} = \frac{\lambda L^2}{h^2 E_{Tf}}$

where L and h are illustrated in Fig. 1 and E_{Tf} is the transverse modulus of elasticity of the face sheet. Six-layer configurations of FGSB are used in this study (Table 1), wherein h_1, h_2, etc are measured from the central layer of SW.

Table 1. Thickness coordinates of different lamination schemes

LS	Thickness coordinates
1-0-1	h_1=-h/2, h_2=0, h_3=0 and h_4=h/2
2-1-2	h_1=-h/2, h_2=-h/10, h_3=h/10 and h_4=h/2
1-1-1	h_1=-h/2, h_2=-h/6, h_3=h/6 and h_4=h/2
1-2-1	h_1=-h/2, h_2=-h/4, h_3=h/4 and h_4=h/2
2-1-1	h_1=-h/2, h_2=-h/4, h_3=0 and h_4=h/2
2-2-1	h_1=-h/2, h_2=-3/10, h_3=h/10 and h_4=h/2

A convergence study was performed for present models (1-2-1), Type P-H (Fig. 5), and Type P-S (Fig. 6) at L/h=5 and n=2 for using different mesh divisions of 4, 8, 16, and 32. As the results converged at a mesh size of 16 so, it is adopted throughout this study. Table 2 presents the buckling response of the FGSW beam for the six lamination schemes and different power law factors. The present results are compared with those reported earlier: Kahya et al [17] used FSDT, Nguyen et al [19] used HOT, Vo et al [21] used refined HOT, Vo et al [28] used quasi-3D theory for getting the responses and the present results are in good agreement with these.

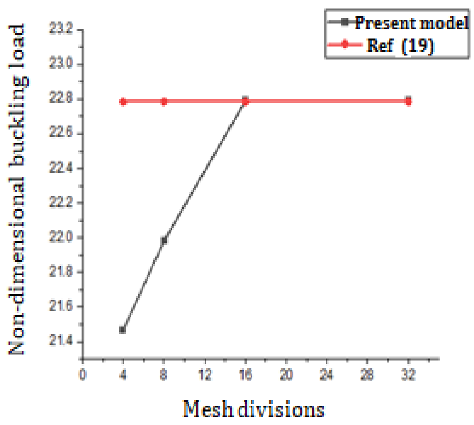

Fig. 5. Variation of buckling load with mesh divisions for a SS 1-2-1 Type P-H FGSW beam

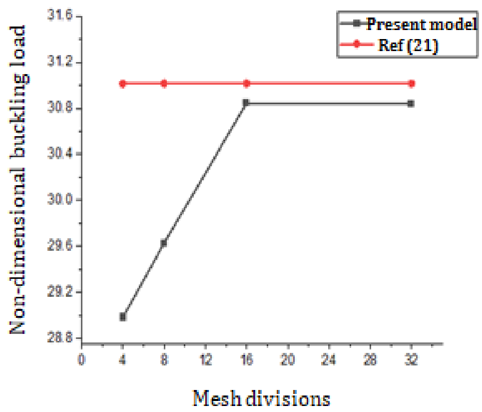

Fig. 6. Variation of buckling load with mesh divisions for a SS 1-2-1 Type P-S FGSW beam

So, the present theory can be applied to buckling solution of FGSW beams. As expected, FSDT results [17] are yielding lower values of non-dimensional buckling load in comparison to all other theories. Beams with lower power-law factors were found to withstand higher buckling loads irrespective of the lamination schemes for both Type-H beams owing to the variation of the material property of FGSW (Fig. 3a, 4a) in the thickness direction, while beams with higher power-law factor were found to withstand higher buckling loads irrespective of lamination schemes for both homogenization rule of Type S owing to the material property variation FGSW (Fig. 3b, 4b).

A high drift in buckling response is seen for a change of 1 unit (0 to 1) in the power law factor, which can be attributed to a change in material properties with a change of the power-law factor (Figs. 3a, 4a). However, for a change of 5 units (5-10) of the power-law, the change in the buckling resistance is found to be very less in comparison to that found an increase of 1 unit of power law factor from 0 to 1. The above-stated variation of buckling resistance with a change in power law factor is valid for both Type S and Type H beams and all lamination schemes considered in the present study. The 1-2-1 lamination scheme was found to have the highest buckling resistance for Type H beams for both homogenization schemes and for all power law factors, which can be attributed to the highest core thickness of the 1-2-1 scheme which is made up of ceramic material. End conditions were also found to have a significant effect on buckling strength.

Table 3 presents the buckling response of Type S FGSW beams for various lamination schemes and power-law factors. With an increase in the power-law factor, an enhanced buckling response is observed (Figs. 3b, 4b) owing to the dependency of the material property on the power-law factor. Lamination scheme 1-0-1 was found to have the highest buckling resistance for Type S beams for both homogenization rules and for all power law factors, which can be attributed to the lowest core thickness made of metal material (having lower strength in comparison to ceramic material). Again, lamination scheme 1-2-1 was found to have the highest buckling resistance among all lamination schemes for type H beams, for both homogenization rules and for all power law factors, which can be attributed to the highest core thickness made of ceramic material (having high strength in comparison to metallic material).

Tables 4 and 5 provide the variation of buckling response with an augment in the aspect ratio of the beam. Tables 4 and 5 are represented again in terms of graphs for greater clarity of the buckling strength variation. The effect of an increase in the length-to-height ratio on buckling response was found to be significant up to a value of 20, after which there was a little change in buckling response for both Type H and S FGSW beams (Figs. 7-12).

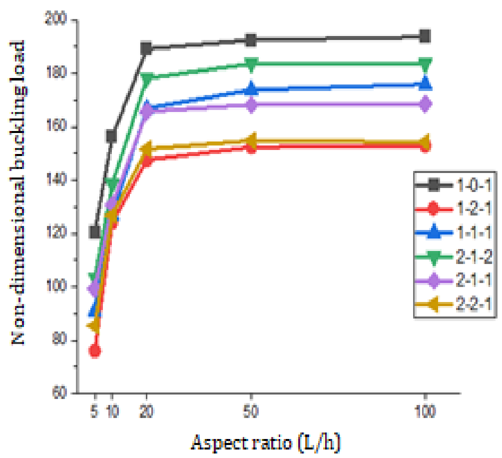

Fig. 7. Variation of buckling load with aspect ratio for Type P-S FGSW beam with the CC end condition

Table 2. Variation of non-dimensional buckling load for Type-H FGSW beam for SS end condition (L/h=5)

LC	n	Present models		Reference solutions			
		Type P-H	Type E-H	Ref. [17]	Ref. [19]	Ref. [21]	Ref. [28]
1-0-1	0	48.592	48.592	48.590	48.596	48.595	49.590
	1	19.658	19.202	19.485	19.654	19.652	20.742
	2	13.586	13.171	13.436	13.582	13.580	13.883
	5	10.240	10.154	10.012	10.148	10.146	10.367
	10	10.530	10.414	9.3292	10.537	9.4515	9.6535
1-2-1	0	48.592	48.592	47.969	48.596	48.595	49.590
	1	28.453	28.062	28.142	28.444	28.444	29.075
	2	22.791	22.429	22.571	22.785	22.786	23.304
	5	18.320	18.004	17.941	18.091	18.091	18.509
	10	16.562	16.073	16.244	16.378	16.378	16.757
1-1-1	0	48.592	48.592	48.152	48.596	48.595	49.590
	1	24.257	23.847	24.326	24.560	24.559	25.107
	2	18.389	18.017	18.190	18.359	18.358	18.777
	5	13.154	13.018	13.583	13.722	13.721	14.035
	10	12.658	12.249	12.112	12.262	12.260	12.539
2-1-2	0	48.592	48.592	48.333	48.596	48.595	49.590
	1	22.684	22.023	22.017	22.212	22.210	22.706
	2	15.417	15.087	15.762	15.916	15.915	16.276
	5	11.658	11.149	11.517	11.669	11.667	11.930
	10	10.581	10.177	10.354	10.537	10.534	10.768
2-1-1	0	48.592	48.592	48.277	48.596	48.595	49.590
	1	23.745	23.129	23.303	23.525	23.524	24.083
	2	17.778	17.033	17.144	17.325	17.324	17.774
	5	13.458	13.171	12.839	13.027	13.027	13.392
	10	11.814	11.128	11.606	11.837	11.838	12.173
2-2-1	0	48.592	48.192	48.130	48.595	48.596	49.590
	1	26.482	26.029	26.108	26.361	26.361	26.976
	2	20.462	19.946	20.186	20.375	20.375	20.887
	5	15.748	15.249	15.572	15.730	15.731	16.160
	10	14.413	14.076	14.027	14.199	14.200	14.599

Table 3. Variation of non-dimensional buckling load for Type-S FGSW beam for SS end condition (L/h=5)

LC	n	Present models		Reference solutions				
		Type P-S	Type E-S	Ref. [21]	CPT [38]	FSDT [38]	TOT [38]	HBT*[38]
1-0-1	0	8.9523	8.9523	8.9519	9.869	8.9508	8.9533	8.9579
	1	36.227	37.897	36.210	42.650	38.252	36.091	35.624
	2	41.86	43.569	42.450	49.207	44.415	42.326	41.293
	5	46.750	49.245	46.650	52.797	48.105	46.574	45.022
	10	46.487	49.271	47.782	53.425	48.918	47.743	46.043
1-2-1	0	8.9523	8.9523	8.9519	9.869	8.9508	8.9533	8.9579
	1	26.475	27.513	26.480	33.089	29.126	26.369	26.491
	2	30.841	32.410	31.015	39.372	34.604	30.793	31.036
	5	34.867	35.487	35.035	44.504	39.192	34.693	35.067
	10	36.427	37.691	36.687	46.356	40.903	36.302	36.722
1-1-1	0	8.9523	8.9523	8.9519	9.869	8.9508	8.9533	8.9579
	1	30.379	32.426	30.244	37.389	33.063	30.064	30.262
	2	35.512	36.692	35.705	44.188	39.139	35.420	35.732
	5	40.216	42.646	40.323	49.184	43.790	39.980	40.354
	10	42.165	43.861	42.069	50.736	45.326	41.733	42.098
2-1-2	0	8.9523	8.9523	8.9519	9.8696	8.9508	8.9533	8.9579
	1	32.912	34.268	32.897	39.940	35.506	32.717	32.914
	2	38.714	39.508	38.858	46.794	41.757	38.615	38.881
	5	43.476	44.228	43.533	51.330	46.137	43.295	43.555
	10	45.253	47.861	45.114	52.514	47.403	44.909	45.132
2-1-1	0	8.9523	8.9523	8.951	-	-	-	-
	1	30.841	32.629	30.931	-	-	-	-
	2	36.387	37.816	36.484	-	-	-	-
	5	40.740	42.486	40.981	-	-	-	-
	10	42.498	43.826	42.600	-	-	-	-
2-2-1	0	8.9523	8.9523	8.952	-	-	-	-
	1	27.554	28.508	27.887	-	-	-	-
	2	32.482	33.419	32.790	-	-	-	-
	5	36.785	37.697	37.035	-	-	-	-
	10	38.617	39.162	38.701	-	-	-	-

Table 4. Variation of non-dimensional buckling load for Type-H FGSW beam at n=2

LC	L/h	CC		CF		SS	
		Type P-H	Type E-H	Type P-H	Type E-H	Type P-H	Type E-H
1-0-1	5	47.725	46.235	3.514	3.501	13.487	13.296
	10	50.579	49.527	3.520	3.516	14.075	13.952
	20	56.283	55.162	3.562	3.546	14.201	14.075
	50	57.621	55.862	3.687	3.636	14.236	14.086
	100	57.694	55.923	3.692	3.667	14.238	14.092
1-2-1	5	78.562	77.625	5.946	5.942	22.768	22.261
	10	86.953	85.361	6.008	5.998	23.741	23.420
	20	94.865	93.142	6.026	6.019	23.974	23.469
	50	95.012	94.267	6.127	6.113	24.043	23.895
	100	95.167	94.323	6.137	6.116	24.057	23.984
1-1-1	5	64.427	63.124	4.761	4.726	18.372	18.159
	10	71.086	70.268	4.792	4.781	19.087	18.946
	20	76.124	75.239	4.831	4.821	19.211	19.027
	50	76.743	75.563	4.891	4.861	19.256	19.082
	100	76.886	75.689	4.885	4.873	19.254	19.087
2-1-2	5	56.241	55.198	4.125	4.023	15.931	15.756
	10	61.845	60.271	4.166	4.110	16.467	16.004
	20	65.861	64.176	4.183	4.142	16.602	16.243
	50	66.279	65.142	4.211	4.189	16.643	16.281
	100	66.386	65.194	4.237	4.206	16.651	16.289
2-1-1	5	60.621	59.297	4.498	4.462	17.324	17.137
	10	63.710	62.581	4.510	4.496	17.627	17.340
	20	71..987	70.371	4.531	4.431	18.142	18.003
	50	72.416	71.892	4.562	4.452	18.206	18.129
	100	72.449	71.709	4.569	4.430	18.427	18.221
2-2-1	5	70.756	69.926	5.296	5.157	20.374	20.164
	10	74.927	73.804	5.324	5.234	20.687	20.531
	20	84.847	83.429	5.368	5.271	21.396	21.082
	50	85.621	84.155	5.372	5.293	21.412	21.210
	100	85.699	84.162	5.376	5.310	21.345	21.261

Table 5. Variation of non-dimensional buckling load for Type-S FGSW beam at n=2

LC	L/h	CC		CF		SS	
		Type P-H	Type E-S	Type P-S	Type E-S	Type P-H	Type E-S
1-0-1	5	120.512	122.629	11.841	11.986	42.312	43.260
	10	156.219	158.210	12.069	12.152	47.351	48.297
	20	189.246	190.856	12.286	12.298	48.702	49.106
	50	192.458	193.071	12.349	12.423	49.165	49.913
	100	193.652	193.303	12.428	12.520	49.191	50.097
1-2-1	5	76.031	77.527	9.234	9.356	31.428	32.568
	10	124.091	125.413	9.532	9.627	36.834	37.201
	20	147.549	148.109	9.831	9.916	38.657	39.644
	50	152.365	153.720	9.843	9.891	39.237	39.923
	100	152.927	153.806	9.982	9.993	39.341	40.108
1-1-1	5	90.947	91.743	10.437	10.861	35.428	36.638
	10	126.879	127.238	10.854	10.985	41.612	42.942
	20	166.940	167.280	11.207	11.305	43.521	44.054
	50	173.830	174.297	11.304	11.356	44.097	44.395
	100	173.894	174.309	11.368	11.413	44.084	44.409
2-1-2	5	103.498	104.986	11.138	11.206	38.715	39.264
	10	138.496	139.207	11.349	11.382	44.537	45.291
	20	178.172	179.206	11.641	11.753	46.281	47.059
	50	183.607	184.283	11.726	11.840	46.725	47.195
	100	183.582	184.782	11.749	11.851	46.741	47.238
2-1-1	5	99.256	100.231	10.467	10.561	36.495	37.951
	10	130.719	132.569	10.561	10.629	39.259	40.192
	20	165.658	166.217	10.745	10.861	42.931	43.187
	50	168.265	169.261	10.835	10.964	43.380	44.014
	100	168.481	169.445	10.890	10.983	43.928	44.464
2-2-1	5	85.379	86.120	9.483	9.496	32.820	33.165
	10	126.843	127.954	9.641	9.692	35.619	36.155
	20	151.667	152.294	9.979	9.986	39.547	40.127
	50	154.831	155.549	9.986	9.992	39.803	40.651
	100	154.271	155.982	9.987	10.107	40.101	40.756

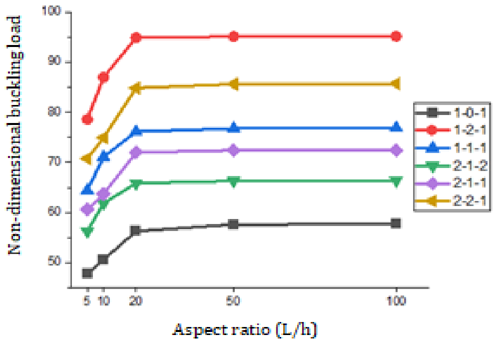

Fig. 8. Variation of buckling load with aspect ratio for Type P-H FGSW beam with the CC end condition

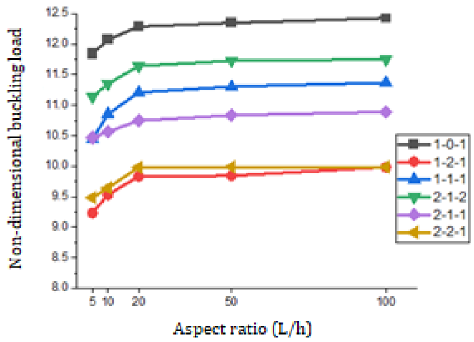

Fig. 9. Variation of buckling load with aspect ratio for Type P-S FGSW beam with CF end condition

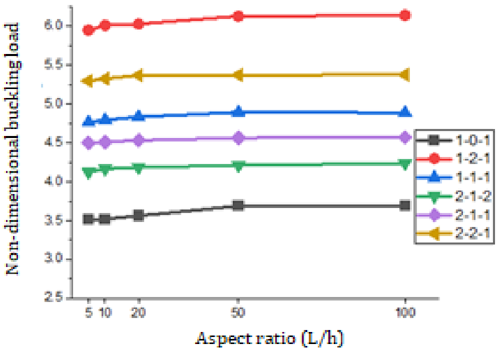

Fig. 10. Variation of buckling load with aspect ratio for Type P-H FGSW beam with CF end condition

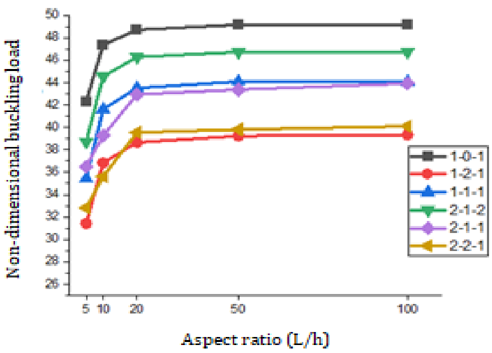

Fig. 11. Variation of buckling load with aspect ratio for Type P-S FGSW beam with the SS end condition

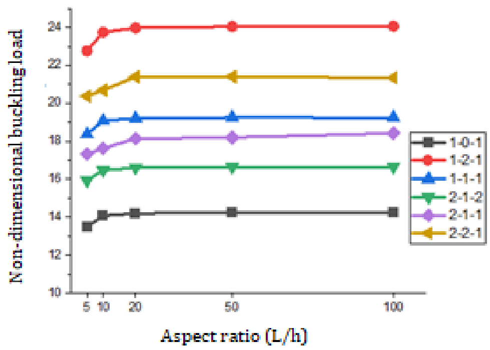

Fig. 12. Variation of buckling load with aspect ratio for Type P-H FGSW beam with SS end condition

6. Conclusions

This paper presents buckling responses of the FGSW beams made of power law and exponential law using zigzag theory. Higher-order terms are assumed for displacement approximations. Numerical results are arrived at by using the FEM of three noded elements having 7DOF/node. The present model is C0 continuous and does not require any post-processing method. The locking phenomenon which is associated with FEM is avoided here. Results of the present model are compared with the existing ones and are found to be consistent, which describes the suitability of the present model in deriving results for FGSW beams. It is found that buckling response is dependent on the power-law factor, aspect ratio, lamination schemes, and end conditions. Many new results are given which will pose as a benchmark for parallel studies. The main inferences drawn from the study are:

1) The buckling strength was improved by increasing the power-law factor for Type S beams while the opposite behavior was seen in type H beams for all types of lamination schemes and end conditions.
2) The end conditions played a major role in deciding the buckling response of FGSW beams.
3) Two types of laws were used in this paper to synthesize the FGM part of FGSW beams. The difference in buckling load resistance on using these two laws is small, but its trend is different for the two types: Type S and Type H.
4) It is found that exponential law-governed FGSW beams show a little higher buckling resistance behavior in comparison to power law-governed FGSW beams for Type S while the opposite behavior is seen for Type H beams for all types of end conditions and lamination schemes.

Acknowledgments

The first author of this paper was financially supported jointly by MHRD, GoI, and Director, NIT Kurukshetra, through a Ph.D. scholarship grant (2K18/NITK/PHD/6180093).

Conflicts of Interest

The author declares that there is no conflict of interest regarding the publication of this manuscript. In addition, the authors have entirely observed the ethical issues, including plagiarism, informed consent, misconduct, data fabrication and/or falsification, double publication and/or submission, and redundancy.

Appendix

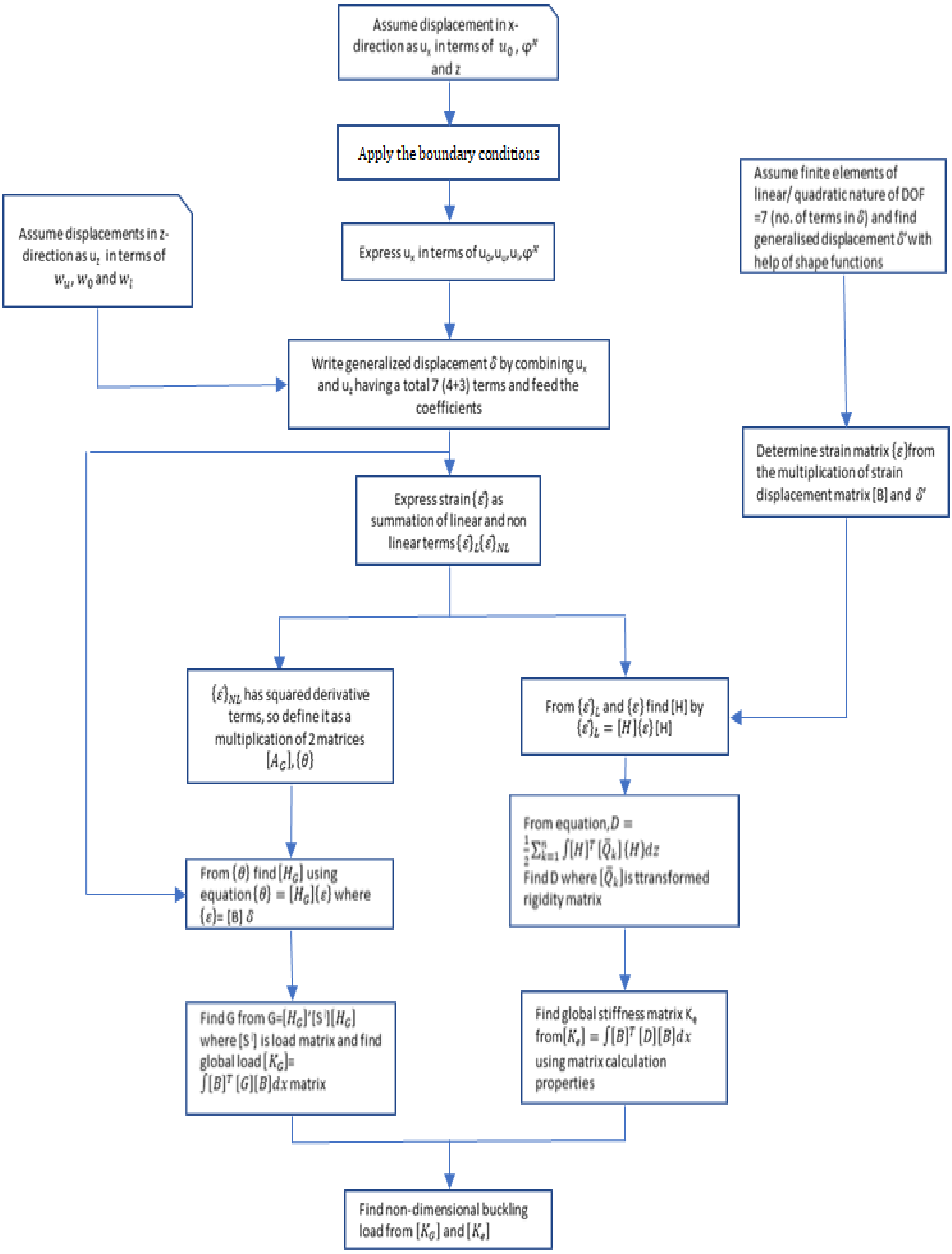

References

[1] Birman, V. and Kardomateas, G.A., 2018. Review of current trends in research and applications of sandwich structures. Composites Part B: Engineering, 142, pp.221-240.

[2] Hemmatian, H., Fereidoon, A., and Shirdel, H., 2014. Optimization of Hybrid Composite Laminate Based on the Frequency using Imperialist Competitive Algorithm. Mechanics of Advanced Composite Structures, 1(1), pp. 37-48.

[3] Torabi, K., Shariati-Nia, M. and Heidari-Rarani, M., 2014. Modal Characteristics of Composite Beams with Single Delamination-A Simple Analytical Technique. Mechanics of Advanced Composite Structures, 1(2), pp.97-106.

[4] Mustapha, S., Ye, L., Wang, D. and Lu, Y., 2011. Assessment of debonding in sandwich CF/EP composite beams using A0 Lamb wave at low frequency. Composite structures, 93(2), pp.483-491.

[5] Sedighi, M., Omidi, N., Jabbari, A., 2017. Experimental Investigation of FGM Dental Implant Properties Made from Ti/HA Composite. Mechanics of Advanced Composite Structures, 4(3), pp.233-237.

[6] Saleh, B., Jiang, J., Fathi, R., Al-hababi, T., Xu, Q., Wang, L., Song, D. and Ma, A., 2020. 30 Years of functionally graded materials: An overview of manufacturing methods, Applications and Future Challenges. Composites Part B: Engineering, 201, pp.108376.

[7] Garg, A., Belarbi, M. O., Chalak, H. D., and Chakrabarti, A., 2021. A review of the analysis of sandwich FGM structures. Composite Structures, 258, pp.113427.

[8] Zhong, Z., and Yu, T., 2007. Analytical solution of a cantilever functionally graded beam. Composites Science and Technology, 67(3-4), pp. 481-488.

[9] Ding, H. J., Huang, D. J., and Chen, W., 2007. Elasticity solutions for plane anisotropic functionally graded beams. International Journal of Solids and Structures, 44(1), pp. 176-196.

[10] Kashtalyan, M., and Menshykova, M., 2009. Three-dimensional elasticity solution for sandwich panels with a functionally graded core. Composite structures, 87(1), pp.36-43.

[11] Celebi, K. E. R. İ. M. C. A. N., and Tutuncu, N., 2014. Free vibration analysis of functionally graded beams using an exact plane elasticity approach. Proceedings of the Institution of Mechanical Engineers, Part C: Journal of Mechanical Engineering Science, 228(14), pp. 2488-2494.

[12] Chu, P., Li, X. F., Wu, J. X., and Lee, K., 2015. Two-dimensional elasticity solution of elastic strips and beams made of functionally graded materials under tension and bending. Acta Mechanica, 226(7), pp. 2235-2253.

[13] Aydogdu, M., and Taskin, V., 2007. Free vibration analysis of functionally graded beams with simply supported edges. Materials & Design, 28(5), pp.1651-1656.

[14] Yang, J., and Chen, Y., 2008. Free vibration and buckling analyses of functionally graded beams with edge cracks. Composite Structures, 83(1), pp.48-60.

[15] Şimşek, M., and Kocatürk, T., 2009. Free and forced vibration of a functionally graded beam subjected to a concentrated moving harmonic load. Composite Structures, 90(4), pp. 465-473.

[16] Su, H., Banerjee, J. R., and Cheung, C. W. (2013). Dynamic stiffness formulation and free vibration analysis of functionally graded beams. Composite Structures, 106, pp. 854-862. DOI: 10.1016/j.compstruct.2013.06.029.

[17] Chakraborty, A., Gopalakrishnan, S., and Reddy, J. (2003). A new beam finite element for the analysis of functionally graded materials. International journal of mechanical sciences, 45(3), pp.519-539.

[18] Pradhan, K. K., and Chakraverty, S., 2013. Free vibration of Euler and Timoshenko functionally graded beams by Rayleigh-Ritz method. Composites Part B: Engineering, 51, pp. 175-184.

[19] Kahya, V., and Turan, M., 2018. Vibration and stability analysis of functionally graded sandwich beams by a multi-layer finite element. Composites Part B: Engineering, 146, pp. 198-212.

[20] Tran, T. T., Nguyen, N. H., Do, T. V., Minh, P. V. and Duc, N. D., 2021. Bending and thermal buckling of unsymmetric functionally graded sandwich beams in high-temperature environment based on a new third-order shear deformation theory. Journal of Sandwich Structures & Materials, 23(3), pp. 906-930.

[21] Nguyen, T. K., Nguyen, T. T. P., Vo, T. P., and Thai, H. T., 2015. Vibration and buckling analysis of functionally graded sandwich beams by a new higher-order shear deformation theory. Composites Part B: Engineering, 76, pp. 273-285.

[22] Daikh, A. A., Guerroudj, M., El Adjrami, M., and Megueni, A., 2020. Thermal buckling of functionally graded sandwich beams. Advanced materials research 1156, pp. 43-59.

[23] Merdaci, S., Hadj Mostefa, A., Beldjelili, Y., Merazi, M., Boutaleb, and S., Hellal, H., 2021. Analytical solution for static bending

analysis of functionally graded plates with porosities, Frattura ed Integrità Strutturale, 55, pp.65-75.

[24] Vo, T. P., Thai, H. T., Nguyen, T. K., Maheri, A., and Lee, J., 2014. Finite element model for vibration and buckling of functionally graded sandwich beams based on a refined shear deformation theory. Engineering structures, 64, pp. 12-22.

[25] Nguyen, T. K., and Nguyen, B. D., 2015. A new higher-order shear deformation theory for static, buckling, and free vibration analysis of functionally graded sandwich beams. Journal of Sandwich Structures & Materials, 17(6), pp.613-631.

[26] Osofero, A. I., Vo, T. P., Nguyen, T. K., and Lee, J., 2016. Analytical solution for vibration and buckling of functionally graded sandwich beams using various quasi-3D theories. Journal of Sandwich Structures & Materials, 18(1), pp.3-29.

[27] Nguyen, T. K., Vo, T. P., Nguyen, B. D., and Lee, J., 2016. An analytical solution for buckling and vibration analysis of functionally graded sandwich beams using a quasi-3D shear deformation theory. Composite Structures, 156, pp.238-252.

[28] Neves, A. M. A., Ferreira, A. J. M., Carrera, E., Cinefra, M., Jorge, R. M. N., Mota Soares, C. M., and Araújo, A. L., 2017. Influence of zig-zag and warping effects on buckling of functionally graded sandwich plates according to sinusoidal shear deformation theories. Mechanics of Advanced Materials and Structures, 24(5), pp.360-376.

[29] Sayyad, A. S., and Avhad, P. V., 2019. On static bending, elastic buckling and free vibration analysis of symmetric functionally graded sandwich beams. Journal of Solid Mechanics, 11(1), pp.166-180.

[30] Sayyad, A. S., and Ghugal, Y. M., 2019. A sinusoidal beam theory for functionally graded sandwich curved beams. Composite Structures, 226, pp.111246.

[31] Vo, T. P., Thai, H. T., Nguyen, T. K., Inam, F., and Lee, J., 2015. A quasi-3D theory for vibration and buckling of functionally graded sandwich beams. Composite Structures, 119, pp. 1-12. DOI: 10.1016/j.compstruct.2014.08.006

[32] Pandey, S., and Pradyumna, S., 2018. Analysis of functionally graded sandwich plates using a higher-order layerwise theory, Composites part B: engineering, 153, pp.325-336.

[33] Averill, R. C., 1994. Static and dynamic response of moderately thick laminated beams with damage. Composites Engineering, 4(4), pp. 381-395.

[34] Cho, Y. B., and Averill, R. C., 1997. An improved theory and finite-element model for laminated composite and sandwich beams using first-order zig-zag sublaminate approximations. Composite Structures, 37(3-4), 281-298.

[35] Filippi, M., and Carrera, E., 2016. Bending and vibrations analyses of laminated beams by using a zig-zag-layer-wise theory. Composites Part B: Engineering, 98, pp. 269-280.

[36] Neves, A. M. A., Ferreira, A. J. M., Carrera, E., Cinefra, M., Jorge, R. M. N., Mota Soares, C. M., and Araújo, A. L., 2017. Influence of zig-zag and warping effects on buckling of functionally graded sandwich plates according to sinusoidal shear deformation theories. Mechanics of Advanced Materials and Structures, 24(5), pp.360-376.

[37] Kapuria, S., Dumir, P. C., and Jain, N. K., 2004. Assessment of zigzag theory for static loading, buckling, free and forced response of composite and sandwich beams. Composite structures, 64(3-4), pp.317-327.

[38] Chakrabarti, A., Chalak, H. D., Iqbal, M., & Sheikh, A. H., 2012. Buckling analysis of laminated sandwich beam with soft core. Latin American Journal of Solids and Structures, 9, pp.1-15.

[39] Iurlaro, L., Gherlone, M., and Di Sciuva, M., 2014. Bending and free vibration analysis of functionally graded sandwich plates using the refined zigzag theory. Journal of Sandwich Structures & Materials, 16(6), pp. 669-699.

[40] Belarbi, M. O., Garg, A., Houari, M. S. A., Hirane, H., Tounsi, A., and Chalak, H. D., 2021. A three-unknown refined shear beam element model for buckling analysis of functionally graded curved sandwich beams. Engineering with Computers, pp.1-28.

[41] Carrera, E., 2003. Historical review of zig-zag theories for multilayered plates and shells. Appl. Mech. Rev., 56(3), pp.287-308.

[42] Kapuria, S., and Ahmed, A., 2019. An efficient zigzag theory based finite element modeling of composite and sandwich plates with multiple delaminations using a hybrid continuity method. Computer Methods in Applied Mechanics and Engineering, 345, pp. 212-232.

[43] Sayyad, A. S., and Ghugal, Y. M., 2020. On the buckling analysis of functionally graded sandwich beams using a unified beam theory. Journal of Computational Applied Mechanics, 51(2), pp.443-453.

[44] Garg, A., Belarbi, M. O., Chalak, H. D., and Chakrabarti, A., 2021. A review of the analysis of sandwich FGM structures, Composite Structures, 258, pp. 113427.

[45] Swaminathan, K., and Sangeetha, D. M., 2017. Thermal analysis of FGM plates–A critical

review of various modeling techniques and solution methods, Composite Structures, 160, pp.43-60.
[46] Najibi, A., and Talebitooti, R., 2017. Nonlinear transient thermo-elastic analysis of a 2D-FGM thick hollow finite length cylinder, Composites Part B: Engineering, 111, pp.211-227.
[47] Najibi, A., 2017. Mechanical stress reduction in a pressurized 2D-FGM thick hollow cylinder with finite length, International Journal of Pressure Vessels and Piping, 153, pp.32-4.